Quadrupole moment of the yrast superdeformed band in ^{144}Gd

C. A. Ur,* D. Bazzacco, G. P. Bolzonella, S. Lunardi, N. H. Medina,† C. M. Petrache,* M. N. Rao,† and C. Rossi Alvarez
Dipartimento di Fisica and INFN, Sezione di Padova, Padova, Italy

L. H. Zhu,‡ G. de Angelis, D. De Acuna, and D. R. Napoli
INFN, Laboratori Nazionali di Legnaro, Legnaro, Italy

W. Gast, R. M. Lieder, and T. Rzaca-Urban§
Institut für Kernphysik, KFA Jülich, Jülich, Germany

R. Wyss
Royal Institute of Technology, Physics Department Frescati, Stockholm, Sweden
(Received 3 June 1999; published 27 September 1999)

A mean lifetime measurement using the Doppler shift attenuation method has been performed at GASP in order to measure the quadrupole moment of the yrast superdeformed band of ^{144}Gd. The extracted intrinsic quadrupole moment above the backbending, $Q_0 = 13.7^{+1.1}_{-0.9}$ e b, is in nice agreement with cranked shell model predictions. To fit the data properly below the backbending a smaller Q_0 value is required $(11.6^{+1.4}_{-1.0})e$ b. This is consistent with the predicted lower deformation in the second well for the configuration without high-N ($\pi N = 6$ and $\nu N = 7$) intruder orbitals occupied. [S0556-2813(99)02210-4]

PACS number(s): 21.10.Re, 21.10.Tg, 23.20.Lv, 27.60.+j

I. INTRODUCTION

The yrast superdeformed (SD) band of ^{144}Gd is one of the few examples of rotational bands built on the second minimum which exhibits a backbending [1,2]. The backbend occurs at a rotational frequency $\hbar\omega = 0.45$ MeV and is explained by the crossing between bands based on configurations with zero and two protons in the $N=6$ $i_{13/2}$ orbital. The observation of the band even below the backbending, where the protons do not occupy the strong deformation driving $i_{13/2}$ orbital, points to a delicate balance between proton and neutron SD-shell gaps that stabilizes above the proton backbend [1,3]. The highly fragmented decay-out of the band, which prevented so far the observation of any linking transitions, speaks in favor of a pronounced difference in deformation between the states built on the first minimum and the SD states below the backbending where 100% of the decay-out occurs. Cranked shell model calculations predict an increase in deformation by about 10% when passing from the $\pi 6^0$ configuration below the backbending ($\beta_2 \approx 0.47$) to the $\pi 6^2$ configuration above the backbend ($\beta_2 \approx 0.51$) [1].

The dependence of the quadrupole deformation on the number of occupied high-N intruder orbitals is well established in the $A=150$ region from lifetime measurements of many superdeformed bands. Of particular relevance, in this respect, are the recent measurements done in ^{148,149}Gd, ^{152}Dy [4], and ^{151,152}Dy, ^{151}Tb [5]. Various theoretical calculations, in the framework of the cranked Nilsson-Strutinsky [6,7], Woods-Saxon-Strutinsky [3], Skyrme-Hartree-Fock [8], and relativistic mean field approaches [9] have been able to predict the dependence of the charge quadrupole moment on the content of high-N intruder orbitals. Very recently, two of these theoretical approaches [8,7] have shown that the relative quadrupole moments of SD bands in the $A=150$ mass region can be written as a sum of independent contributions from the single-particle–hole states around the doubly magic superdeformed core ^{152}Dy. The configuration of the yrast SD band of ^{144}Gd above the backbending differs from that of ^{152}Dy by two $N=6$ protons and six neutrons (four $N=6$ and two $N=7$). Since the ^{144}Gd nucleus is also considered to be doubly magic at superdeformed shapes, it is very interesting to test whether the additivity of single particle quadrupole moments holds from one doubly magic nucleus to another.

We report in this paper on a Doppler shift attenuation method (DSAM) lifetime measurement for the yrast SD band of ^{144}Gd performed with the goal to test the predictive power of current theories with respect to the deformation driving contribution of specific high-N orbitals. A preliminary report of our results has been presented elsewhere [10].

II. DSAM LIFETIME EXPERIMENT AND DATA ANALYSIS

Superdeformation in ^{144}Gd has been studied previously by our group using the ^{100}Mo+^{48}Ti reaction at three different bombarding energies [2] and the ^{74}Ge+^{74}Ge reaction at 318 MeV [11]. Despite the relative higher population of the yrast SD band obtained in the ^{74}Ge+^{74}Ge reaction, the ^{100}Mo+^{48}Ti reaction at 214 MeV has been preferred because of the higher beam current available in this second

*On leave from Institute of Physics and Nuclear Engineering, Bucharest, Romania.

†On leave from Instituto di Física, Universidade de São Paulo, São Paulo, Brazil.

‡On leave from China Institute of Atomic Energy, Beijing, China.

§On leave from Warsaw University, Warsaw, Poland.

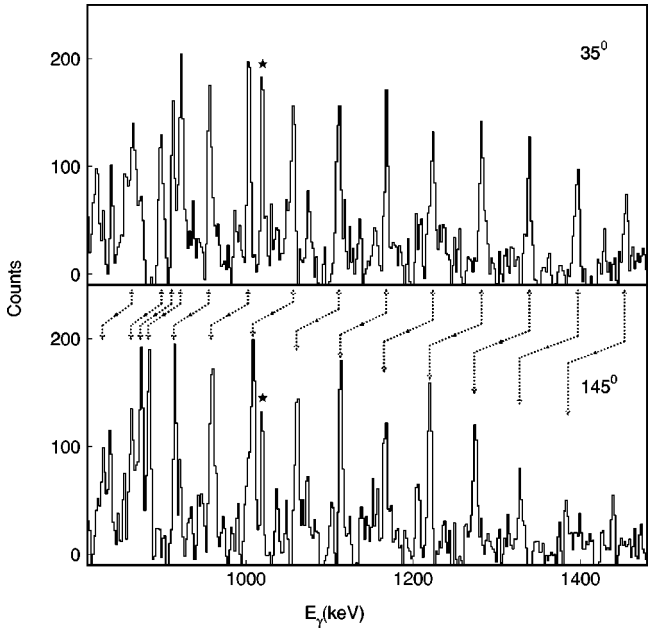

FIG. 1. Double-gated coincidence spectra corresponding to the detectors of the 35° and 145° rings with respect to the beam direction. Gates are set on clean transitions belonging to the ^{144}Gd yrast SD band. The shifts of the γ rays are indicated by arrows. The line marked with an asterisk corresponds to the 1018 keV $12^+ \rightarrow 10^+$ transition in the low-spin part of the level scheme.

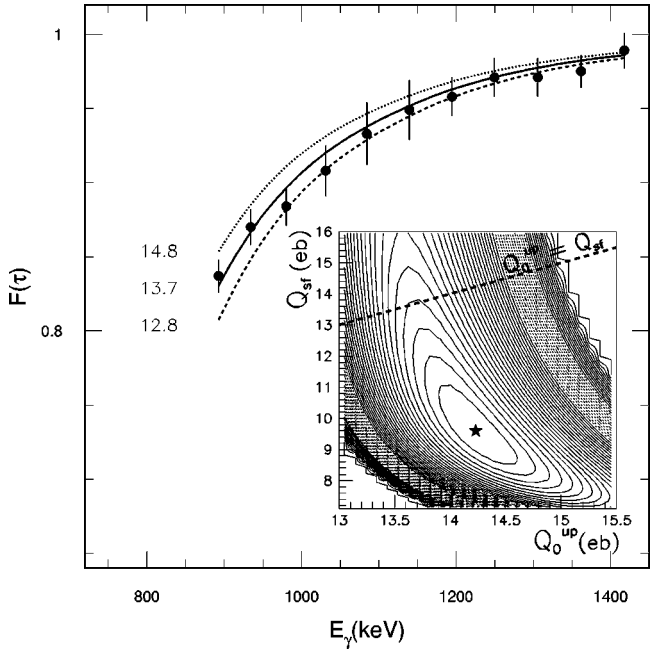

FIG. 2. Experimental (filled circles) fractional Doppler shifts for γ-ray transitions depopulating states of the ^{144}Gd SD band above the backbending. Tha data are taken from the spectra corresponding to the most forward and backward rings of detectors. The solid line represents the best fit to the data when keeping the same value for the SD band and the side-feeding quadrupole moments leading to $Q_0 = 13.7$ *e* b. The limits to the Q_0 value as obtained by a standard χ^2 minimization procedure are also drawn. The inset shows the two-dimensional χ^2 minimization surface as a function of Q_0 and $Q_{\rm sf}$. The star represent the absolute minimum in the surface whereas the dashed line corresponds to $Q_0 = Q_{\rm sf}$.

case. The beam was delivered by the XTU Tandem accelerator of the Legnaro National Laboratories. The target consisted of a 1 mg/cm^2 ^{100}Mo foil evaporated on a 10 mg/cm^2 gold backing which completely stops the recoiling nuclei. γ rays were detected by the GASP array consisting of 40 high efficiency Compton-suppressed HPGe detectors and of an inner ball of 80 bismuth germanate (BGO) detectors. Events were collected when at least 3 suppressed Ge detectors and five BGO detectors of the inner ball fired in coincidence. A total of 2.13×10^9 events were collected on tape, which, after the data unpacking resulted in 3.94×10^9 threefold coincidence events available for off-line analysis.

The Ge detectors in the GASP array are placed symmetrically with respect to the beam direction in seven rings, as follows: six at 35°, six at 60°, four at 72°, eight at 90°, four at 108°, six at 120°, and six at 145°. In the off-line analysis the highest spin states of ^{144}Gd (including SD states) were enhanced by setting proper conditions (high sum-energy and high multiplicity) on the inner BGO ball. In order to simplify the analysis, the data were reduced by sorting only the events with energy comprised between 750 and 1625 keV, which corresponds to the region where the SD band transitions lie. The analyzed spectra were obtained by double gating on in-band transitions seen by all detectors and projecting on the seven rings of detectors available in the GASP geometry. Typical double-gated spectra at forward and backward angles are shown in Fig. 1.

The experimental fractional Doppler shift, $\mathrm{F}(\tau)$, was determined according to the following relation:

$$F(\tau) = \frac{\Delta E_\gamma}{2\beta E_{\gamma 0} \cos\theta_{\rm fwd}}, \tag{2.1}$$

where ΔE_γ is the energy difference between the centroids of the shifted γ rays corresponding to the forward and backward angles ($\theta_{\rm fwd}$ and $\pi - \theta_{\rm fwd}$, respectively), $E_{\gamma 0}$ is the unshifted γ-ray energy, and $\beta = v_0/c$, where v_0 is the mean initial recoil velocity. The resulting $\mathrm{F}(\tau)$ values versus the energy of the SD band transitions are presented in Figs. 2 and 3; the error bars drawn in the figure are the statistical errors derived from the spectra of the 35° and 145° detectors. The points corresponding to the 1084 and 1134 keV transitions are taken only from the forward ring, since these transitions are strongly contaminated in the backward ring.

The slowing down process of the recoiling nuclei and the velocity profile have been simulated using the codes developed by Bacelar *et al.* [12], as modified by Gascon *et al.* [13]. The stopping power and the multiple scattering of the recoils were described using a Monte Carlo simulation based on the LSS parametrization [14]. We used a number of 5000 histories and up to 1600 steps of 1 fs. The electronic stopping power was calculated according to the formalism of Braune [15]. The calculation of the theoretical $F(\tau)$ values depends on the mean decay time of the state (often called

''apparent lifetime''), which is defined by the mean lifetime of the state and the entire decay history above the state, including the unknown sidefeeding. The program we used is a modified version of the one reported in Ref. [4] and is dealing with a rotational cascade, having a constant intrinsic quadrupole moment Q_0, where each state has a sidefeeding provided by a rotational sideband with the same dynamical moment of inertia $\mathfrak{I}^{(2)}$ as the SD band and an intrinsic quadrupole moment Q_{sf}.

The assumption is furthermore made that all sidebands feeding the SD band levels have the same $Q_{\rm sf}$, as suggested previously by Ref. [16] and measured more recently [4] for this mass region. Since the cranked shell model calculations (see Introduction) predict a configuration change associated with the backbending, we have chosen to fit separately the data points above and below the backbending. In the following we will therefore denote by Q_0^{up} the intrinsic quadrupole moment of the states above the backbending and by Q_0^{do} the one for the states below the backbending. It is clear that the analysis will be more accurate for the states above the backbending where a larger number of experimental points is available.

The intensity of the sidefeeding was taken from a previous measurement using thin target [2] and recalculated according to the double gating procedure employed to build the spectra. For a better description of the in-band decay history we took into account in the calculations all four γ-ray transitions above the one of 1418 keV, the last one for which we could measure the $F(\tau)$ value (see Fig. 1). The side-feeding effects are stronger in the upper part of the SD band where the side-feeding intensities are large compared with the in-band decay. In order to reproduce the side-feeding effects the program allows to add on top of the SD band a cascade of virtual γ-ray transitions having the same $J^{(2)}$ as the SD band and a quadrupole moment $Q_{\rm sf}$. In our case, the best fit of the data was obtained by adding a cascade of three virtual γ-ray transitions on top of the known SD band transitions.

In the inset of Fig. 2 we show the two-dimensional minimization of the χ^2 values in the space defined by Q_0^{up} and $Q_{\rm sf}$. One can notice the large covariance between Q_0^{up} and $Q_{\rm sf}$ which results in a wide minimum. The absolute minimum χ^2 value correspond to $Q_0^{up}=14.2$ e b and $Q_{\rm sf}=9.6$ e b (that point is marked with a star on the figure). This would imply a slow sidefeeding which is not consistent with the data since the apparent lifetime of the highest levels of the SD band is very short (about 10 fs or less). The same situation has been encountered in the case of the yrast SD band in ^{152}Dy [16] and, following that work, we have also assumed that the side-feeding bands have the same feeding history as the SD band leading to equal values for the side feeding and effective in-band feeding times. This assumption is also supported by a more recent work on several neighboring nuclei [4]. In order to derive the SD band quadrupole moment we have then followed the $Q_0^{up}=Q_{\rm sf}$ line marked in the inset of Fig. 2 by a dashed line. The minimum χ^2 value corresponds to $Q_0^{up}=13.7^{+1.1}_{-0.9}$ e b. The calculated F(τ) curves for the best fit of the experimental data and for the error limits are also shown in Fig. 2 together with the experimental points.

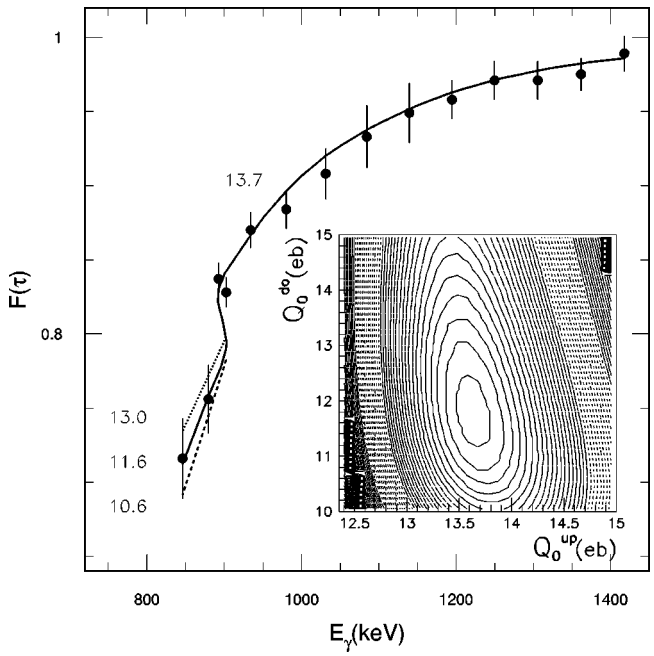

FIG. 3. Experimental (filled circles) fractional Doppler shifts for the whole yrast SD band in ^{144}Gd extracted from the spectra corresponding to the most forward and backward ring of detectors. The solid line represents the best fit to the data with the corresponding Q_0 values above and below the backbending indicated. The limits to the Q_0 value below the backbending as obtained by a standard χ^2 minimization procedure are also drawn. The inset shows the two-dimensional χ^2 minimization surface as a function of Q_0^{up} and Q_0^{do}.

Once obtained in this way the quadrupole moment of the SD band above the backbending we extended the analysis to include also the points below the backbending. In the inset of Fig. 3 we show the two-dimensional minimization of the χ^2 values in the space defined by Q_0^{up} and Q_0^{do}. The minimum value correspond to $Q_0^{up}=13.7$ e b (with practically the same error limits as from the analysis of the points above the backbending) and $Q_0^{do}=11.6^{+1.4}_{-1.0}$ e b. We also show in Fig. 3 the $F(\tau)$ curve calculated for the entire band with $Q_0^{up}=13.7$ e b and $Q_0^{do}=11.6$ e b and the limits defined by the errors on the Q_0^{do}.

The errors on the final values of Q_0 both above and below the backbending, as obtained from the χ^2 minimization procedure, are rather large. This implies that the two Q_0 values overlap at 12.8–13.0 e b and a unique Q_0 of about 13.0 e b along the whole band could also fit the data. This gives on the other side a much higher χ^2 and we therefore believe that the data are indicative of a decrease of the quadrupole moment when going from states above to states below the backbending. If we take the values corresponding to the best fit of the data ($Q_0^{up}=13.7$ e b, $Q_0^{do}=11.6$ e b) a 15% change in deformation is derived. A drop of collectivity (but not quantified) has been also reported for the SD band 2 in ^{149}Gd below the backbending observed at low frequencies [4].

We have also to note that the results are, as usual, subject to 10–15 % systematic errors due to the uncertainties on the stopping power parametrizations. However, this does not affect the relative deformations below and above the backbending.

III. DISCUSSION

The quadrupole moment of the yrast SD band of ^{144}Gd has been calculated by cranked Strutinsky type calculations based on an average Woods-Saxon potential with a monopole pairing force [3]. The calculated value of $Q_0 = 13.5$ (3) e b for the configuration $\pi 6^2 \nu 7^0$ is in excellent agreement with our experimental value above the backbending.

The calculations of Ref. [3] have been later on improved by treating deformation and pairing self-consistently [1,17]. The results of these calculations yield $Q_0 = 12.5$ e b and $Q_0 = 13.9$ e b below and above the backbending, respectively [1].

In the present work, we have further improved the parameters of the Woods-Saxon potential and extended the pairing force to include both monopole and quadrupole components. (For details concerning the method, see Ref. [18].) The quadrupole moment of a specific configuration is calculated microscopically from the expectation values of the Q_{20} and Q_{22} operators at the minimum of the total Routhian surface. The backbend in the calculations is considerably smoother than in experiment (see also Ref. [1]). This is related to a shortcoming of the cranking model, when a mixing between a zero and two quasiparticle configuration occurs at a given frequency. The quadrupole moment above the backbend yields at $\hbar\omega = 0.5(0.8)$ MeV a value of 13.2 (12.9) e b for the $\langle Q_{20} \rangle$ operator and 1.1 (1.8) e b for $\langle Q_{22} \rangle$, resulting in a total value of 14.3 (14.7) e b. In contrast, below the backbend, the quadrupole moment is calculated to have a value of 12.7 e b at $\hbar\omega = 0.25$ MeV. We have taken a rather low value of the rotational frequency, in order to avoid the region where the $\pi 6^0$ and the $\pi 6^2$ configurations are mixed in the calculations. The absolute value of the calculated quadrupole moment depends on the uncertainties related to the proton charge radius of the Woods-Saxon potential, but the relative changes between different configurations should be accounted for by the model. We note an increase of $\approx 11\%$ in the quadrupole moment when going from the $\pi 6^0 \nu 7^0$ to the aligned $\pi 6^2 \nu 7^0$ configuration, that agrees rather well with the experimental estimate. This corresponds to a calculated (experimental) effective quadrupole moment change of $\delta Q = 1.6$ e b (2.1 e b) for the $\pi([660]1/2)^2$ configuration.

As discussed previously [1], our calculations yield a change in the structure of the yrast band in the second well from predominantly $\pi 6^0 \nu 7^0$ to $\pi 6^2 \nu 7^0$ in the aligned band. Note, however, that these particle-hole assignments are rather schematic, since pairing correlations are still present which induce the partial occupation and mixing of the two configurations. The doubly magic shell closure at $N = 80$ and $Z = 64$ becomes effective only after the proton alignment, where the occupation of the strongly downsloping $N = 6$ $\pi i_{13/2}$ orbital opens up the proton shell gap at a similar deformation as the neutron shell gap, thus stabilizing the superdeformed shape (see Fig. 5 in Ref. [2] and the general discussion in Ref. [19]). It is thus the combined effect of shell structure (shell-gaps) and polarization, that results in the increased deformation after the proton backbending.

As mentioned in the Introduction, different theoretical approaches are successful in reproducing many properties of SD bands, in particular their quadrupole moments. The cranked Nilsson-Strutinsky and cranked relativistic mean field approaches have been applied for systematic investigations of SD rotational bands in the $A \approx 140-150$ mass region. They both yield a Q_0 value of ≈ 13.8 e b for the yrast SD band of ^{144}Gd band above backbending [7,9], a value which is in excellent agreement with our experimental result. However, these theoretical analyses do not quote any value of the quadrupole moment for the yrast SD band of ^{144}Gd below the backbend.

IV. CONCLUSIONS

We have measured the deformation along the yrast SD band of ^{144}Gd by means of the DSAM technique and deduced quadrupole moments of $Q_0 = 11.6^{+1.4}_{-1.0}$ e b and $Q_0 = 13.7^{+1.1}_{-0.9}$ e b below and above the backbending, respectively. This result is nice agreement with theoretical calculations which predict a change in configuration from $\pi 6^0$ to $\pi 6^2$ for the yrast SD band and the corresponding increase of its quadrupole moment. The stabilization of the $Z = 64$ and $N = 80$ SD shell gaps occurs therefore at enhanced deformation.

ACKNOWLEDGMENTS

We are indebted to the technical staff of L. N. L. for the careful operation of the Tandem accelerator. A. Buscemi, R. Isocrate, and R. Zanon are thanked for their skillful help in the preparation of the experiments at GASP. N.H.M. and M.N.R. acknowledge partial support from the Fundação de Amparo à Pesquisa do Estado de São Paulo (FAPESP) and the Conselho Nacional de Desenvolvimento Científico e Tecnológico (CNPq), Brazil. T.R.Z. was partially supported by KBN Grant No. 2P03B 05312.

[1] S. Lunardi, D. Bazzacco, C. Rossi Alvarez, P. Pavan, G. de Angelis, D. De Acuna, M. De Poli, G. Maron, J. Rico, O. Stuch, D. Weil, S. Utzelmann, P. Hoernes, W. Satuła, and R. Wyss, Phys. Rev. Lett. **72**, 1427 (1994).

[2] S. Lunardi, L. H. Zhu, C. M. Petrache, D. Bazzacco, N. H. Medina, M. A. Rizzuto, C. Rossi Alvarez, G. de Angelis, G. Maron, D. R. Napoli, S. Utzelmann, W. Gast, R. M. Lieder, A. Georgiev, F. Xu, and R. Wyss, Nucl. Phys. **A618**, 238 (1997).

[3] W. Nazarewicz, R. Wyss, and A. Johnson, Nucl. Phys. **A503**, 285 (1989).

[4] H. Savajols, A. Korichi, D. Ward, D. Appelbe, G. C. Ball, C. Beausang, F. A. Beck, T. Byrski, D. Curien, P. Dagnall, G. de France, D. Disdier, G. Duchene, S. Erturk, C. Finck, S. Flibotte, B. Gall, A. Galindo-Uribarri, B. Haas, G. Hackman, V. P. Janzen, B. Kharraja, J. C. Lisle, J. C. Merdinger, S. M. Mullins, S. Pilotte, D. Prevost, D. C. Radford, V. Rauch, C.

Rigollet, D. Smalley, M. B. Smith, O. Stezowski, J. Styczen, Ch. Theisen, P. J. Twin, J. P. Vivien, J. C. Waddigton, K. Zuber, and I. Ragnarsson, Phys. Rev. Lett. **76**, 4480 (1996).

[5] D. Nisius, R. V. F. Janssens, E. F. Moore, P. Fallon, B. Crowell, T. Lauritzen, G. Hackman, I. Ahmad, H. Amro, S. Asztalos, M. P. Carpenter, P. Chowdhury, R. M. Clark, P. J. Daly, M. A. Deleplanque, R. M. Diamond, S. M. Fischer, Z. W. Grabowski, T. L. Khoo, I. Y. Lee, A. O. Macchiavelli, R. H. Mayer, F. S. Stephens, A. V. Afanasjev, and I. Ragnarsson, Phys. Lett. B **392**, 18 (1997).

[6] T. Bengtsson, S. Aberg, and I. Ragnarsson, Phys. Lett. B **208**, 39 (1988).

[7] L. B. Karlsson, I. Ragnarsson, and S. Aberg, Nucl. Phys. **A639**, 654 (1998).

[8] W. Satuła, J. Dobaczewski, J. Dudek, and W. Nazarewicz, Phys. Rev. Lett. **77**, 5182 (1996).

[9] A. V. Afanasjev, J. König, and P. Ring, Nucl. Phys. **A608**, 107 (1997).

[10] C. A. Ur, G. P. Bolzonella, L. H. Zhu, D. Bazzacco, S. Lunardi, N. H. Medina, C. M. Petrache, M. N. Rao, C. Rossi Alvarez, G. de Angelis, D. De Acuna, D. R. Napoli, W. Gast, R. M. Lieder, T. Rzaca-Urban, S. Utzelmann, and R. Wyss, *Proceeding of the Conference on Nuclear Structure at the Limits*, ANL/PHY-97/1, Argonne National Laboratory, 1996 (unpublished), p. 84.

[11] L. H. Zhu, M. Cinausero, S. Lunardi, G. Viesti, D. Bazzacco, G. de Angelis, M. De Poli, D. Fabris, E. Fioretto, A. Gadea, F. Lucarelli, M. Lunardon, N. H. Medina, D. R. Napoli, C. M. Petrache, G. Prete, and C. Rossi Alvarez, Nucl. Phys. **A635**, 325 (1998).

[12] J.C. Bacelar, R. M. Diamond, E. M. Beck, M. A. Deleplanque, J. Draper, and F. S. Stephens, Phys. Rev. C **35**, 1170 (1987).

[13] J. Gascon, C.-H. Yu, G. B. Hagemann, M. C. Carpenter, J. M. Espino, Y. Iwata, T. Komatsubara, J. Nyberg, S. Ogaza, G. Sletten, P. O. Tiom, D. C. Radford, J. Simpson, A. Alderson, M. A. Bentley, P. Fallon, P. D. Forsyth, J. W. Roberts, and J. F. Sharpey-Schafer, Nucl. Phys. **A513**, 344 (1990).

[14] J. Lindhard, M. Scharff, and H.E. Schiott, Mat. Fys. Medd. K. Dan. Vidensk. Selsk. **33**, 1 (1963) as presented in the paper of W. M. Curie, Nucl. Instrum. Methods Phys. Res. **73**, 173 (1969).

[15] K. Braune, MPI Heidelberg Diploma, 1977; D. Pelte and D. Schwalm, in *Heavy Ion Collisions*, edited by R. Bock (North-Holland, Amsterdam, 1982), Vol. 3, Chap. 1.

[16] M. A. Bentley, A. Alderson, G. C. Ball, H. W. Cranmer-Gordon, P. Fallon, B. Fanta, P. D. Forsyth, B. Herskind, D. Howe, C. A. Kalfas, A. R. Mokhtar, J. D. Morrison, A. H. Nelson, B. M. Nyako, K. Schiffer, J. F. Sharpey-Schafer, J. Simpson, G. Sletten, and P. J. Twin, J. Phys. G **17**, 481 (1991).

[17] W. Satuła, R. Wyss, and P. Magierski, Nucl. Phys. **A578**, 45 (1994).

[18] W. Satuła and R. Wyss, Phys. Scr. **T56**, 159 (1995).

[19] R. Wyss, J. Nyberg, A. Johnson, R. Bengtsson, and W. Nazarewicz, Phys. Lett. B **215**, 211 (1988).